The Journal of Experimental Biology 215, 1306-1312

doi:10.1242/jeb.066605

RESEARCH ARTICLE

Active echolocation beam focusing in the false killer whale, *Pseudorca crassidens*

Laura N. Kloepper*, Paul E. Nachtigall, Megan J. Donahue and Marlee Breese
Hawaii Institute of Marine Biology, University of Hawaii, PO Box 1106, Kailua, HI 96734, USA
*Author for correspondence (kloepper@hawaii.edu)

Accepted 19 December 2011

SUMMARY

The odontocete sound production system is highly complex and produces intense, directional signals that are thought to be focused by the melon and the air sacs. Because odontocete echolocation signals are variable and the emitted click frequency greatly affects the echolocation beam shape, investigations of beam focusing must account for frequency-related beam changes. In this study we tested whether the echolocation beam of a false killer whale changed depending on target difficulty and distance while also accounting for frequency-related changes in the echolocation beam. The data indicate that the false killer whale changes its beam size according to target distance and difficulty, which may be a strategy of maximizing the energy of the target echo. We propose that the animal is using a strategy of changing the focal region according to target distance and that this strategy is under active control.

Key words: echolocation, beam focusing, odontocete.

INTRODUCTION

Toothed whales and dolphins possess many adaptations that make them well suited to an aquatic environment, including the use of echolocation and the development of high-frequency hearing and sound production. Odontocetes have evolved structures to effectively produce high-frequency signals and transmit them into the water. The odontocete nasal anatomy is highly complex, consisting of muscles, fatty tissues, and a network of air sacs (Schenkkan, 1973; Mead, 1975; Cranford et al., 1996; Houser et al., 2004). These nasal passages are homologous to those of terrestrial mammals (Klima, 1987), and the muscles surrounding these passages are derived from the m. maxillonasolabialis, a facial muscle found in some terrestrial mammals (Huber, 1934; Lawrence and Schevill, 1956; Schenkkan, 1973; Mead, 1975). Norris et al. (Norris et al., 1961) first proposed the idea that odontocete echolocation sounds may be generated in the forehead region and transmitted to the water in a directional beam. Since this seminal study, much investigation has been conducted regarding sound generation in odontocetes.

To generate echolocation clicks, odontocetes produce short, ultrasonic signals with pneumatically driven pulses generated in the nasal complex and subsequently focused into a directional signal (Ridgway et al., 1980; Mackay and Liaw, 1981; Cranford, 1992; Aroyan et al., 2000; Au et al., 2006). The nasal structures directly responsible for pulse generation are two structures called the monkey lips dorsal bursae (MLDB) complex (Cranford et al., 1996). Each MLDB complex consists of a valve containing dense connective tissue (the phonic lips) that contains a pair of fat bodies (the dorsal bursae) surrounded by a thin pouch of connective tissue (Cranford et al., 1996). Prior to pulse emission, air is sent from the lungs to the bony nasal passage, with a corresponding increase in air pressure within this cavity (Dormer, 1974; Ridgway et al., 1980; Cranford et al., 2011). During an echolocation event, air is forced upward and past the MLDB complex (Dormer, 1974; Ridgway et al., 1980). The air travels between the phonic lips and causes them to slap together, creating the echolocation pulses (Cranford et al., 1996; Cranford et al., 2011). Odontocetes possess two sets of MLDB complexes and may use one or both to produce echolocation pulses (Lammers and Castellote, 2009; Madsen et al., 2010; Cranford et al., 2011).

Structures within the forehead of odontocetes help direct the sound towards the anterior portion of the forehead and may focus the echolocation beam (Evans et al., 1964). The portion of the skull lying directly posterior to the MLDB complex is concave in most odontocetes and is composed of highly dense bone (Mead, 1975). Air spaces cover this portion of the skull and act as acoustic reflectors for the pulses generated by the MLDB (Aroyan et al., 1992; Au et al., 2010; Cranford et al., 2011). The pressure and size of these air sacs change over the course of an echolocation event, which may result in differential reflection of the echolocation pulses (Dormer, 1974; Ridgway et al., 1980). The melon, a structure filled with acoustic fats and located anterior of the air sacs, may further focus the emitted pulses. Although the size, shape and lipid composition of the melon differs across genera (Litchfield et al., 1973; Cranford et al., 1996), the presence of acoustic fats in the forehead is common to all odontocetes. The distribution and layering of fats inside the melon act to focus the sound towards the anterior portion of the melon and act as an impedance-matching device for sounds traveling into the surrounding seawater (Litchfield et al., 1973; Norris and Harvey, 1974; Malins and Varanasi, 1975). Additionally, the melon is surrounded and traversed by a complex array of muscles and tendons that may act to change the shape of the melon during echolocation (Harper et al., 2008). It is hypothesized that the animal may control the size and shape of the air sacs and melon to differentially focus the echolocation beam, although such active focusing has yet to be demonstrated empirically.

Early investigations with odontocetes hinted at the directionality of their echolocation signals (Norris et al., 1961; Evans et al., 1964; Norris and Evans, 1966), which prompted measurement of the

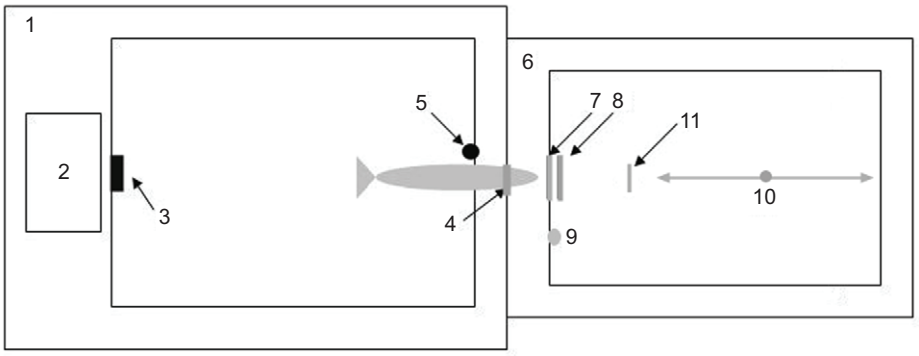

Fig. 1. Experimental setup. 1, Experimental pen; 2, experimental shack; 3, stationing pad; 4, hoop; 5, response paddle; 6, target pen; 7, acoustically opaque screen; 8, visual screen; 9, monitoring camera; 10, targets (position varied between 2.5, 4 and 7 m); 11, recording hydrophone array. Grey represents objects located underwater; black represents objects located above water.

transmission beam patterns (Evans, 1973). Beam patterns have been directly measured under laboratory conditions for *Tursiops truncatus* (Au et al., 1978; Au et al., 1980; Au et al., 1986), *Delphinapteus leucas* (Au et al., 1987), *Pseudorca crassidens* (Au et al., 1995) and *Phocoena phocoena* (Au et al., 1999), and have been estimated from field recordings of *Lagenorhynchus albirostris* (Rasmussen at al., 2004), *Platanista gangetica* (Bahl et al., 2007), *Physeter macrocephalus* (Mohl et al., 2003) and *Ziphius cavirostris* (Zimmer et al., 2005a). Most odontocete signals measured thus far have 3 dB beamwidths (the angle at which the beam's power is half the maximum power of the signal) between 8 and 15 deg, with interspecific and intraspecific variation (Au, 1993).

Odontocetes demonstrate flexibility and adaptability with their echolocation. They change the frequency and intensity of their signals as a result of environmental or hearing changes (Au et al., 1985; Ibsen et al., 2007; Kloepper et al., 2010a), and can change the shape or direction of their echolocation beam (Au et al., 1987; Moore et al., 2008). Changes in beam width have previously been thought to be frequency driven; that is, beam size is determined primarily by the laws of linear acoustics in which, for a directional source, higher frequencies create narrower beam patterns (Au et al., 1995). If odontocete beam patterns change solely according to the frequency of the emitted signal, then, for a given frequency, the beam area should be the same regardless of target condition. If, however, after controlling for this frequency effect on beam area, the beam size changes depending on target condition, then the animal may be actively focusing the emitted beam.

In this study, we investigated the adaptability of odontocete echolocation by testing whether the echolocation beam area of a false killer whale changed depending on target difficulty and distance. Accounting for expected differences in beam area with frequency, the false killer whale changed the shape of its echolocation beam, which suggests active focusing of the emitted beam. Based on these data, we propose that the animal changes the size of its beam for difficult echolocation tasks and adjusts the focal region of the beam according to target distance to maximize the amount of energy reflected from the target.

MATERIALS AND METHODS

The experiment was conducted at the floating pen complex of the Marine Mammal Research Program of the Hawaii Institute of Marine Biology off Coconut Island, Kaneohe Bay, Oahu, Hawaii, with a female false killer whale [*Pseudorca crassidens* (Owen 1846)] named Kina. The exact age of the whale is unknown; she was brought to Hawaii as an adult in 1987. In 2010, the subject measured 3.96 m and weighed 540 kg. The setup for the experiment is shown in Fig. 1. During the experiment, the subject stationed in a hoop located 1 m below the surface of the water. An underwater camera (SCS Enterprises, Montebello, NY, USA) was used to monitor her hoop behavior. An acoustically opaque metal screen was located in front of the animal to prevent her from echolocating prematurely on the targets. An acoustically transparent, yet visually opaque polyethylene screen was placed in front of the acoustically opaque screen to ensure that the subject was not utilizing visual cues.

The subject performed a target wall thickness discrimination task similar to that described in Kloepper et al. (Kloepper et al., 2010b). At the start of a trial, the subject remained stationed on a vertically placed pad on the side of the pen near the trainer. When cued, the whale swam into a hoop up to its pectoral fins to remain stationary for the trial. A target was placed into the water using a custom device designed to eliminate potential cuing effects. This V-shaped device allowed each target to be deployed at the same location and depth so that the animal was cuing off of the characteristics of the target and not the target location. After the target was lowered into the water the acoustically opaque screen was moved to reveal the target. The subject ensonified the target and determined whether it was a standard target or a comparison target. If the target was a standard target (a 'go'), the subject backed out of the hoop and touched a response paddle with her rostrum. If the target was a comparison target (a 'no-go'), the subject remained in the hoop until signaled out by the trainer. The subject was rewarded with fish for correct responses. Incorrect responses resulted in no fish reward. Thus, the general form of the procedure was a go/no-go paradigm (Schusterman, 1980).

The standard target was a hollow aluminum cylinder 12.7 cm long with an outer diameter of 37.85 mm and a wall thickness of 6.35 mm. The cylinders were hollow, allowing them to fill with water when submerged. Two comparison targets were used, an 'easy' target and a 'hard' target [prior performance on targets were 98 and 75% correct at 8 m distance, respectively (Kloepper et al., 2010b)]. The comparison targets had the same length and outer diameter as the standard target. The 'easy' target had an inner wall thickness 0.813 mm thicker than the standard, and the 'hard' target had an inner wall thickness 0.203 mm thicker than the standard.

Targets were hung at 1 m depth and at three distances from the animal's blowhole: 2.5, 4 and 7 m. Each session consisted of 50 trials, and each session contained one target type at one distance (e.g. session 1 was 'easy' at 2.5 m, session 6 was 'hard' at 7 m). A total of nine sessions were conducted in an A/B/A format: three sessions with the 'easy' targets (2.5, 4 and 7 m), three sessions with the hard targets (2.5, 4 and 7 m) and three sessions with the 'easy' targets (2.5, 4 and 7 m).

Clicks were recorded using an array of 16 Reson 4013 hydrophones (Reson, Slangerup, Denmark) located 2 m from the blowhole of the animal at a depth of 1 m (Fig. 2). The array

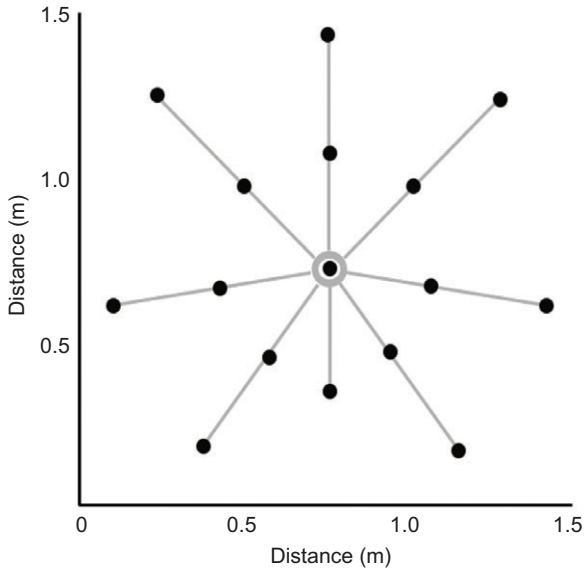

Fig. 2. Diagram and dimensions of the 16-element hydrophone array. Each solid black circle represents the location of a single hydrophone.

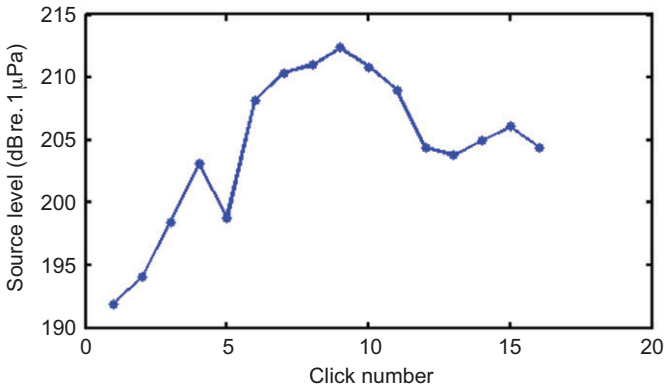

Fig. 3. Pattern of source level (dB re. 1 μPa) *versus* click number, which is stereotypical of click trains from the subject. The figure represents an example click. Echolocation trains begin with low-amplitude pulses and increase in amplitude until a maximal intensity is reached. Following the peak, signal amplitude drops off rapidly.

measured 146 cm in diameter, with hydrophones located approximately 25 cm apart. Each hydrophone occupied an independent channel and was amplified by 20 dB using a custom-built 16 channel amplifier. The signals were sent to a National Instruments DAQmx-PCI 6133 A/D board (Austin, TX, USA) that digitized the signal of each channel at a sample rate of 1 MHz for off-line analysis.

Although stationed in a hoop, the animal had some ability to move its head and corresponding echolocation beam, so analysis was restricted to clicks where the on-axis portion was located on the inner hydrophones of the array. Signals with the measured axis on peripheral hydrophones were omitted because of the possibility of the true on-axis being located off the array. To determine the on-axis, the sound pressure level at each hydrophone in the array was calculated for each click, and the hydrophone with the highest sound pressure level was characterized as the on-axis click. The center frequency, as defined previously (Au, 1993), was calculated for each on-axis click. To determine the beam area for each click, the following procedure was used in a MATLAB program (MathWorks, Natick, MA, USA). First, the sound pressure levels received at each hydrophone on the array were calculated using peak-to-peak voltage. Then, using cubic interpolation from the known hydrophone values (Forsythe et al., 1977), sound pressure levels were estimated on a 0.05 m mesh grid superimposed on the array. From the mesh grid values, a contour characterized by 3 dB less than the on-axis source level was constructed and the area of the contour was calculated using the polyarea function in MATLAB.

The whale produced one click train of multiple echolocation signals in each trial. During a typical click train, the subject's source levels followed a stereotypical pattern, starting at low source levels, increasing to a maximum, and then decreasing towards the end of the click train (Fig. 3). This pattern is common for echolocating odontocetes (Au et al., 1974; Au et al., 1987) and is thought to be a result of the pneumatic generating process (Norris and Harvey, 1972; Dormer, 1979; Ridgway et al., 1980; Amundin and Andersen, 1983). The whale also used a scanning motion with her head and echolocation beam, clicking first off-axis, then directly on the target, and again scanning off-axis. Because the clicks in the middle of her echolocation train were on-axis and at the highest source levels (Fig. 3), the five clicks with the highest source levels from each train were chosen for analysis. The beam area and center frequency for these five clicks were averaged to create a single observation per trial. In total, 99 (2.5 m), 111 (4 m) and 106 (7 m) 'easy' target click trains and 50 (2.5 m), 49 (4 m) and 57 (7 m) 'hard' target click trains were included in the analysis.

We used a general linear model (Rutherford, 2001) to test for the effect of distance and difficulty on beam area, while accounting for the known effect of center frequency on beam area. All analyses were performed in SPSS v.19 (IBM, Armonk, NY, USA). To better satisfy the homoscedasticity assumption of the general linear model, a Box–Cox power transformation (λ=–0.624) was applied to the beam area values for all analyses (Sokal and Rohlf, 1995). To facilitate comparison of the marginal means across treatments, center frequencies from each click train were centered around the mean of all click trains (Vittinghoff et al., 2005). All figures are plotted on the natural (non-transformed) scale for ease of interpretation. The A/B/A format resulted in an unbalanced design with twice as many 'easy' targets as 'hard' targets. We used Type III sums of squares in our analysis, which is specially designed to handle unbalanced designs by calculating the reduction in error sums of squares after all other effects are adjusted (Shaw and Mitchell-Olds, 1993). Unlike Type I and Type II sums of squares, Type III sums of squares are unaffected by sample size. We tested for interactions of treatment with center frequency using the full model: beam area ~ center frequency + difficulty + distance + (center frequency × difficulty) + (center frequency × distance) + (distance × difficulty) + (center frequency × distance × difficulty). Finding no interactions with center frequency (i.e. homogeneity of slopes across treatments, P>0.05 for all interactions with center frequency), we fit the reduced model: beam area ~ center frequency + difficulty + distance + (difficulty × distance). We refer to this homogeneous slopes model as an analysis of covariance (ANCOVA) (Rutherford, 2001). To illustrate the effects of distance and difficulty while controlling for center frequency, we plot the marginal means (Rutherford, 2001). These marginal means were compared using parametric bootstrapping to decrease the risk of Type I error inflation due to unequal sample sizes.

Work was approved under the University of Hawaii Institutional Animal Care Committee Protocol 93-005-15.

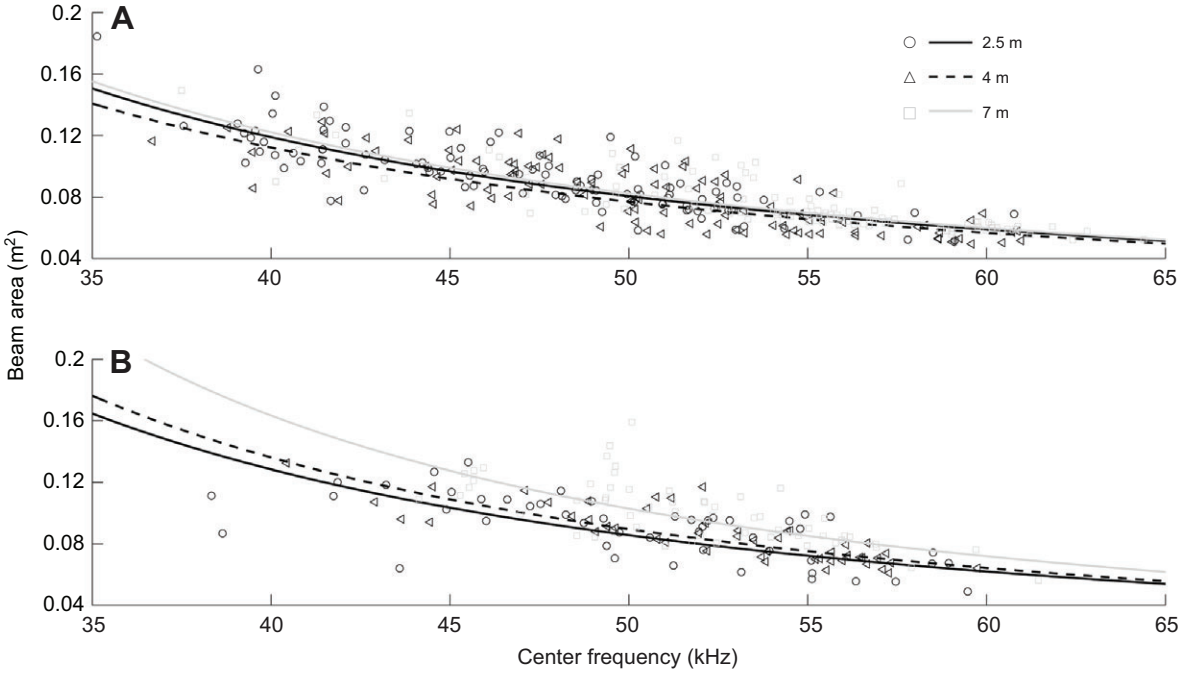

Fig. 4. Scatterplot of beam area *versus* center frequency according to target distance for (A) 'hard' targets and (B) 'easy' targets. Each data point represents the average of the five highest source level values for each click train. Both target sets demonstrate a negative relationship between beam area and center frequency regardless of target distance. Solid lines represent the fitted ANCOVA model for each condition, back-transformed to the natural scale. The grey line and grey squares represent the data for the 7 m target distance, the black dotted line and black triangles represent the data for the 4 m target distance, and the black solid line and black circles represent the data for the 2.5 m target distance.

RESULTS

As expected, beam area decreased with increasing center frequency across all target conditions ($F_{1,465}$=791.9, P<0.005; Fig. 4). Beam areas were larger for difficult targets (difficulty: $F_{1,465}$=10.1, P<0.005) and increased as the distance to the target increased (distance: $F_{1,465}$=22.2, P<0.005), but the pattern differed between target types (difficulty×distance: $F_{1,465}$=22.2, P<0.005; Fig. 5). Averaged across all distances, beam areas were 113% larger for 'hard' targets than 'easy' targets. For 'hard' targets, the marginal mean beam area increased consistently with distance (beam area increased 117% from 2.5 to 7 m), although 2.5 m and 4.0 m were statistically indistinguishable based on bootstrapped 95% confidence intervals. For 'easy' targets, marginal mean beam area increased 96% from 4 to 7 m, whereas the 2.5 m distance was intermediate and statistically indistinguishable from either based on 95% bootstrapped confidence intervals.

DISCUSSION

There was a negative relationship between beam area and center frequency for all target conditions: for each kilohertz the center frequency increased, the beam area decreased by 0.0017 m^2 (Fig. 4). This relationship was consistent across target conditions, as indicated by similar slopes between beam area and center frequency across treatments. This is in agreement with past beam pattern studies (Au et al., 1995) and properties of linear acoustics in which higher frequencies create narrower beams for directional transducers. Because the center frequencies were not evenly distributed over distances and difficulties, the whale tended to use somewhat different frequencies for different tasks. Centering the center frequencies and comparing marginal mean beam areas across target conditions allows comparison of the beam areas while accounting for the effect of frequency. Thus, the ANCOVA results indicate that the changes in beam area according to target condition could not be explained by frequency changes alone. Accounting for frequency, the whale produces wider beam areas for targets that are more difficult to discriminate. Additionally, the beam area widens with increasing distance for the 'hard' targets, but only widens between 4 and 7 m for the 'easy' targets.

If the changes in beam area could not be explained by changes in the frequency content of the outgoing signals, what else could have been changing the beam area? Although the odontocete sound generating system is often modeled as a flat circular piston (Au,

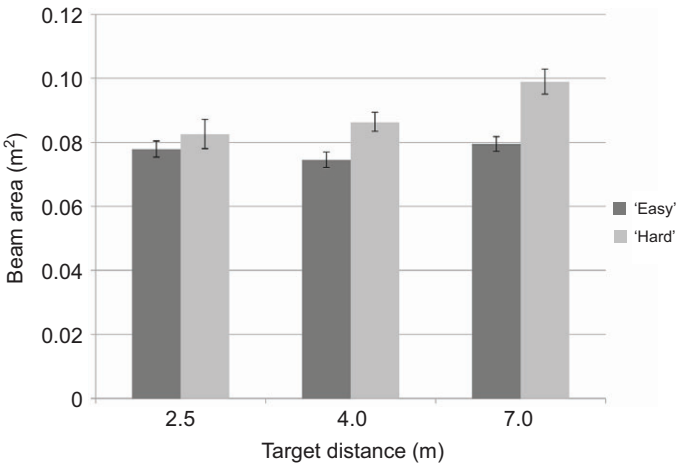

Fig. 5. Beam area (m^2) according to target distance (m) and difficulty. The beam area represents the marginal mean beam area value across all frequencies for each target condition. Beam areas are larger for difficult targets and increase with increasing target distance. The error bars represent the standard error for each marginal mean value.

1993), there are anatomical structures that influence the outgoing echolocation beam and modify the beam area. The dorsal anterior portion of the skull and associated air sacs form a concave shape within the forehead of some odontocetes (Cranford et al., 1996). Because the MLDB complex is located just dorsal and anterior to these structures, it is possible that the skull and air sacs reflect the pulse and the collective structures may function like a spherically concave focusing radiator (O'Neil, 1949). Many devices, such as ultrasound transducers, use spherically concave radiators to create a highly focused beam (Chen et al., 1993). Such a system results in a focused beam so long as the diameter of the radiator is much larger than the wavelength of the emitted signal.

The diameter of the posterior portion of the false killer whale skull is approximately 30 cm (Cowley, 1944) and the wavelength of this species' echolocation signals is approximately 5 cm (Kloepper et al., 2010a). Although there are no published data on the curvature of the *Pseudorca* skull, it is clearly concave (Fig. 6). Thus, assuming that the skull and air sacs reflect the pulses generated in the MLDB complex, the morphology of a false killer whale's sound-generating apparatus might be modeled as a focused radiator that creates a region of very narrow beamwidth at a certain distance from the source (O'Neil, 1949; Chen et al., 1993). Of course, such a simplified model assumes a homogenous volume within the concavity and does not account for the muscles, tissue and acoustic fats that comprise the odontocete forehead and may further modify the echolocation beam. The shape and properties of the melon may act similarly to an optical biconvex lens to further focus the echolocation beam (Keating, 2002), and this focusing may be changed by the muscles surrounding the melon, which are hypothesized to change its shape (Harper et al., 2008).

At first, the results of a narrower beam for easier and closer targets seem counter-intuitive. However, it is important to point out that the size of the beam is from the perspective of the array located 2 m away, not at the actual target. We propose that the increase in beam area measured by our array is due to the animal actively adjusting its focal region according to the target difficulty or distance. When the focal region is narrowed or brought closer to the animal, the beam measured at a fixed distance is smaller than when the focal region is widened or moved farther away from the animal (Fig. 7). Thus, an increase in beam area as measured by the array results in a smaller beam area at the location of the target.

Differentially focusing the emitted beam according to target difficulty or distance can improve the target resolution properties of the odontocete's sonar system and improve foraging capabilities. By creating a focal region of concentrated sound intensity, the animal can maximize the energy reflected back from a prey item and minimize unwanted echoes from clutter objects. The difference in beam size according to target difficulty indicates the animal requires a smaller beam (or wider as measured at the point of our array) for discriminating difficult targets. The 'hard' target is at the behavioral discrimination threshold for the animal (Kloepper et al., 2010b), so the whale is likely maximizing the abilities of its echolocation system. Additionally, the whale changes its beam area according to the distance of the difficult target. Minimizing the size of the echolocation beam for difficult targets located at different distances would result in an increased amount of echo information to aid in better discrimination. Changing the focal region according to target distance may also help increase auditory processing capabilities and improve foraging capabilities by cuing the animal to 'pay attention to' targets at a certain distance along its acoustic axis. This is also supported by observations in training sessions where the animal could not immediately detect a target when moved from 8 m to 2.5 m distance mid-session, and attention has been shown to be a crucial factor in detecting target distance (Penner, 1980). If the animal's auditory system is 'gated' to a specific target distance, it can further enhance auditory processing by ignoring unwanted echoes. This strategy of range-dependent attention is found in bats that change the length of their echolocation calls according to target range (Surlykke et al., 2009; Falk et al., 2011) and in dolphins with varying performance depending on expectation of targets presented at a particular distance (Penner, 1980). Instead of changing the length of their echolocation calls, odontocetes may be using a strategy of changing the focal length of their echolocation beam. Because the data do not indicate a consistent relationship between beam size and distance for the easier targets, this strategy may not be necessary for easy target detection or discrimination tasks. Of course, regardless of beam focus, near targets would produce strong echoes, so it is likely the odontocete auditory system uses further mechanisms for range-dependent processing.

This adjustment of focal region may be caused or controlled by the air sacs (the radiator), the melon (the lens) or both. The complex air sacs lying forward of the dorsal anterior portion of the skull may be differentially inflated to change the shape of the concave portion of the head. Modifications in the shape of the air sacs may change the radius of curvature of the sound reflection structures, which may also change the focusing of the emitted beam. After sound production, further adjustments to the focal region may also be initiated by muscles surrounding the melon, which change the shape of the melon and affect its radius of curvature. The steeper the convex surface, the closer the focal region. Thus, the focal region can be shifted away by elongating the melon in the horizontal plane or compressing the melon in the vertical plane.

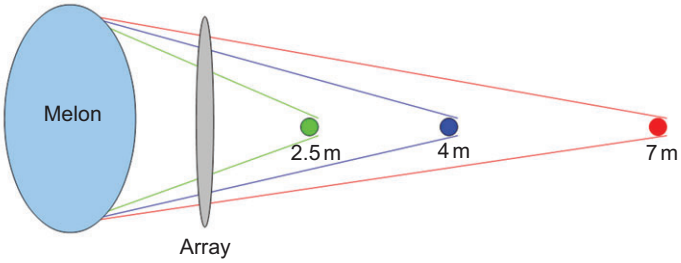

Fig. 7. Schematic of proposed focusing mechanism that would result in increased beam areas measured at the site of the array. Beam areas would appear to increase if the subject is adjusting her focal region according to the distance of the target.

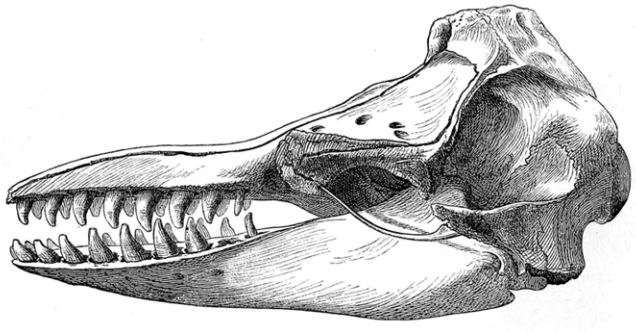

Fig. 6. Sketch of *Pseudorca* skull, showing the concave posterior portion, which may help to focus the emitted beam. From Reinhardt (Reinhardt, 1866).

Of course, until one can look inside an actively echolocating odontocete, any anatomical explanation for beam focusing can only be assessed with models. Regardless of the anatomical structures responsible for focusing the beam, these data show that the odontocete echolocation beam is dynamic and is focused by the animal during echolocation. This focusing is independent of frequency, changes depending on target distance, and target difficulty, and suggests that echolocation beam focusing is under active control by the animal.

ACKNOWLEDGEMENTS

The authors thank all the members of the Marine Mammal Research Program group, including Alexander Supin and Whitlow Au, for their continuous assistance. The authors also thank Ted Cranford, Peter Cameron and two anonymous reviewers for comments on an earlier version of the manuscript, and Michael Weise and Neil Abercrombie for their ongoing support. This is contribution no. 1487 from the Hawaii Institute of Marine Biology.

FUNDING

This research project was supported by the Office of Naval Research (grant NOO14-08-1-1160 to P.E.N.).

REFERENCES

Amundin, M. and Andersen, S. H. (1983). Bony nares air pressure and nasal plug muscle activity during click production in the harbor porpoise, *Phocoena phocoena*, and the bottlenosed dolphin, *Tursiops truncatus*. *J. Exp. Biol.* **105**, 275-282.

Aroyan, J. L., Cranford, T. W., Kent, J. and Norris, K. S. (1992). Computer modeling of acoustic beam formation in *Delphinus delphis*. *J. Acoust. Soc. Am.* **92**, 2539-2545.

Aroyan, J. L., McDonald, M. A., Webb, S. C., Hildebrand, J. A., Clark, D., Laitman, J. T. and Reidberg, J. S. (2000). Acoustic models of sound production and propagation. In *Hearing by Whales and Dolphins* (ed. W. W. L. Au, A. N. Popper and R. R. Fay), pp. 409-469. New York: Springer.

Au, W. W. L. (1980). Echolocation signals of the Atlantic bottlenose dolphin (*Tursiops truncatus*) in open waters. In *Animal Sonar Systems* (ed. R. G. Busnel and J. F. Fish), pp. 251-282. New York, Plenum.

Au, W. W. L. (1993). *The Sonar of Dolphins*, pp. 98-137. New York: Springer-Verlag.

Au, W. W. L., Floyd, R. W., Penner, R. H. and Murchison, A. E. (1974). Measurement of echolocation signals of the Atlantic bottlenose dolphin, *Tursiops truncatus* Montagu, in open water. *J. Acoust. Soc. Am.* **56**, 1280-1290.

Au, W. W. L., Floyd, R. W. and Haun, J. E. (1978). Propagation of Atlantic bottlenose dolphin echolocation signals. *J. Acoust. Soc. Am.* **64**, 411-422.

Au, W. W. L., Carder, D. A., Penner, R. H. and Scronce, B. L. (1985). Demonstration of adaptation in beluga whale echolocation signals. *J. Acoust. Soc. Am.* **77**, 726-730.

Au, W. W. L., Moore, P. W. B. and Pawloski, D. (1986). Echolocation transmitting beam of the Atlantic bottlenose dolphin. *J. Acoust. Soc. Am.* **80**, 688-691.

Au, W. W. L., Penner, R. H. and Turl, C. W. (1987). Propagation of beluga echolocation signals. *J. Acoust. Soc. Am.* **82**, 807-813.

Au, W. W. L., Pawloski, D., Nachtigall, P. E., Blonz, M. and Gisiner, R. (1995). Echolocation signals and transmission beam pattern of a false killer whale (*Pseudorca crassidens*). *J. Acoust. Soc. Am.* **98**, 51-59.

Au, W. W. L., Kastelein, R. A., Rippe, T. and Schooneman, N. M. (1999). Transmission beam pattern and echolocation signals of a harbor porpoise (*Phocoena phocoena*). *J. Acoust. Soc. Am.* **106**, 3699-3705.

Au, W. W. L., Kastelein, R. A., Benoit-Bird, K. J., Cranford, T. W. and McKenna, M. F. (2006). Acoustic radiation from the head of echolocating harbor porpoises (*Phocoena phocoena*). *J. Exp. Biol.* **209**, 2726-2733.

Au, W. W. L., Houser, D. S., Finneran, J. J., Lee, W. J., Talmadge, L. A. and Moore, P. W. (2010). The acoustic field on the forehead of echolocating Atlantic bottlenose dolphins (*Tursiops truncatus*). *J. Acoust. Soc. Am.* **128**, 1426-1434.

Bahl, R., Sugimatsu, H., Kojima, J., Ura, T., Behera, S., Inoue, T. and Fukuchi, T. (2007). Beam pattern estimation of clicks of a free-ranging Ganges river dolphin. *Oceans* **2007**, 1-6.

Chen, X., Schwarz, K. Q. and Parker, K. J. (1993). Radiation pattern of a focused transducer: a numerically convergent solution. *J. Acoust. Soc. Am.* **94**, 2979-2991.

Cowley, L. F. (1944). The skull of the false killer dolphin, *Pseudorca crassidens* (Owen). *Proc. Zool. Soc. Lond.* **114**, 382-387.

Cranford, T. W. (1992). *Functional Morphology of the Odontocete Forehead: Implications for Sound Generation*. PhD dissertation, University of California, Santa Cruz.

Cranford, T. W., Amundin, M. and Norris, K. (1996). Functional morphology and homology in the odontocete nasal complex: implications for sound generation. *J. Morphol.* **228**, 223-285.

Cranford, T. W., Elsberry, W. R., Van Bonn, W. G., Jeffress, J. A., Chaplin, M. S., Blackwood, D. J., Carder, D. A., Kamolnick, T., Todd, M. A. and Ridgway, S. H. (2011). Observation and analysis of sonar signal generation in the bottlenose dolphin (*Tursiops truncatus*): evidence for two sonar sources. *J. Exp. Mar. Biol. Ecol.* **407**, 81-96.

Dormer, K. J. (1974). *The Mechanism of Sound Production and Measurement of Sound Processing in Delphinid Cetaceans*. PhD dissertation, University of California, Los Angeles.

Dormer, K. J. (1979). Mechanisms of sound production and air recycling in delphinids: cineradiographic evidence. *J. Acoust. Soc. Am.* **65**, 229-239.

Evans, W. E. (1973). Echolocation by marine delphinids and one species of fresh-water dolphin. *J. Acoust. Soc. Am.* **54**, 191-199.

Evans, W. E., Sutherland, W. W. and Beil, R. G. (1964). The directional characteristics of delphinid sounds. In *Marine Bio-acoustics,* Vol. 2 (ed. W. N. Tavolga), pp. 353-372. New York: Pergamon Press.

Falk, B., Williams, T., Aytekin, M. and Moss, C. F. (2011). Adaptive behavior for texture discrimination by the free-flying big brown bat, *Eptesicus fuscus*. *J. Comp. Physiol. A* **197**, 491-503.

Forsythe, G. E., Malcolm, M. A. and Moler, C. B. (1977). *Computer Methods for Mathematical Computations,* pp. 70-79. Englewoods Cliffs, NJ: Prentice Hall.

Harper, C. J., McLellan, W. A., Rommel, S. A., Gay, D. M., Dillaman, R. M. and Pabst, D. A. (2008). Morphology of the melon and its tendinous connections to the facial muscles in bottlenose dolphins (*Tursiops truncatus*). *J. Morphol.* **269**, 820-839.

Houser, D. S., Finneran, J., Carder, D., Van Bonn, W., Smith, C., Hoh, C., Mattrey, R. and Ridgway, S. (2004). Structural and functional imaging of bottlenose dolphin (*Tursiops truncatus*) cranial anatomy. *J. Exp. Biol.* **207**, 3657-3665.

Huber, E. (1934). Anatomical notes on Pinnipedia and Cetacea. In *Marine Mammals. Contributions to Paleontology*, no. 447 (ed. E. L. Packard, R. Kellogg and E. Huber), pp. 105-136. Washington, DC: Carnegie Institute of Washington.

Ibsen, S. D., Au, W. W. L., Nachtigall, P. E., DeLong, C. M. and Breese, M. (2007). Changes in signal parameters over time for an echolocating Atlantic bottlenose dolphin performing the same target discrimination task. *J. Acoust. Soc. Am.* **122**, 2446-2450.

Keating, M. P. (2002). *Geometric, Physical, and Visual Optics*, pp. 99-123. Woburn, MA: Butterworth-Heinemann.

Klima, M. (1987). Morphogenesis of the nasal structures of the skull in toothed whales (Odontoceti). In *Morphogenesis of the Mammalian Skull (Mammalia depicta)* (ed. H.-J. Kuhn and U. Zeller), pp. 105-121. Berlin: Parey.

Kloepper, L. N., Nachtigall, P. E. and Breese, M. (2010a). Change in echolocation signals with hearing loss in a false killer whale (*Pseudorca crassidens*). *J. Acoust. Soc. Am.* **128**, 2233-2237.

Kloepper, L. N., Nachtigall, P. E., Gisiner, R. and Breese, M. (2010b). Decreased echolocation performance following high-frequency hearing loss in the false killer whale (*Pseudorca crassidens*). *J. Exp. Biol.* **213**, 3717-3722.

Lammers, M. O. and Castellote, M. (2009). The beluga whale produces two pulses to form its sonar signal. *Biol. Lett.* **5**, 297-301.

Lawrence, B. and Schevill, W. E. (1956). The functional anatomy of the delphinid nose. *Bull. Mus. Comp. Zool.* **114**, 103-151.

Litchfield, C., Karol, R., Mullen, M. E., Dilger, J. P. and Luthi, B. (1979). Physical factors influencing refraction of the echolocative sound beam in delphinid cetaceans. *Mar. Biol.* **52**, 285-290.

Mackay, R. S. and Liaw, C. (1981). Dolphin vocalization mechanisms. *Science*. **212**, 676-678.

Madsen, P. T., Wisniewska, D. and Beedholm, K. (2010). Single source sound production and dynamic beam formation in echolocating harbour porpoises (*Phocoena phocoena*). *J. Exp. Biol.* **213**, 3105-3110.

Malins, D. C. And Varanasi, U. (1975). Cetacean biosonar: Part 2. The biochemistry of lipids in acoustic tissues. In *Biochemical and Biophysical Perspectives in Marine Biology* (ed. D. C. Malins and J. R. Sargent), pp. 237-287. New York: Academic Press.

Mead, J. G. (1975). Anatomy of the external nasal passages and facial complex in the Delphinidae (Mammalia: Cetacea). *Smithson. Contrib. Zool.* **207**, 1-35.

Mohl, B., Wahlberg, M. and Madsen, P. T. (2003). The monopulsed nature of sperm whale clicks. *J. Acoust. Soc. Am.* **114**, 1143-1154.

Moore, P. W., Dankiewicz, L. A. and Houser, D. S. (2008). Beamwidth control and angular target detection in an echolocating bottlenose dolphin (*Tursiops truncatus*). *J. Acoust. Soc. Am.* **124**, 3324-3332.

Norris, K. S. and Evans, W. E. (1966). Directionality of echolocation clicks in the rough-toothed porpoise, *Steno bredanensis* (Lesson). In *Marine Bioacoustics* (ed. W. Tavolga), pp. 305-316. New York: Pergamon Press.

Norris, K. S. and Harvey, G. W. (1972). A theory for the function of the spermaceti organ of the sperm whale (*Physeter catodon* L). In *Animal Orientation and Navigation* (ed. S. R. Galler, K. Schmidt-Koenig, G. J. Jacobs and R. E. Belleville), pp. 397-417. Washington, DC: NASA.

Norris, K. S. and Harvey, G. W. (1974). Sound transmission in the porpoise head. *J. Acoust. Soc. Am.* **56**, 659-664.

Norris, K. S., Prescott, J. H., Asa-Dorian, P. V. and Perkins, P. (1961). An experimental demonstration of echolocation behavior in the porpoise, *Tursiops truncatus* (Montagu). *Biol. Bull* **120**, 163-176.

O'Neil, H. T. (1949). Theory of focusing radiators. *J. Acoust. Soc. Am.* **21**, 516-526.

Penner, R. (1980). Attention and detection in dolphin echolocation. In *Animal Sonar: Processes and Performance* (ed. P. E. Nachtigall and P. W. B. Moore), pp. 707-714. New York: Plenum Press.

Rasmussen, M. H., Wahlberg, M. and Miller, L. A. (2004). Estimated transmission beam pattern of clicks recorded from free-ranging white-beaked dolphins (*Lagenorhynchus albirostris*). *J. Acoust. Soc. Am.* **116**, 1826-1831.

Reinhardt, J. (1866). On *Pseudorca crassidens*. In *Recent Memoirs on the Cetacea* (ed. W. H. Flower), 312 pp. London: Ray Society.

Ridgway, S. H., Carder, D. A., Green, R. F., Gaunt, A. S., Gaunt, S. L. L. and Evans, W. E. (1980). Electromyographic and pressure events in the nasopharyngeal system of dolphins during sound production. In *Animal Sonar Systems* (ed. R. G. Busnel and J. F. Fish), pp. 239-250. New York, Plenum.

Rutherford, A. (2001). *Introducing ANOVA and ANCOVA: a GLM Approach*. London: SAGE Publications.

Schenkkan, E. J. (1973). On the comparative anatomy and function of the nasal tract in odontocetes (Mammalia: Cetacea). *Bijd. Dierkd.* **43**, 127-159.
Schusterman, R. (1980). Behavioral methodology in echolocation by marine mammals. In *Animal Sonar Systems* (ed. R. G. Busnel and J. F. Fish), pp. 11-41. New York: Plenum.
Shaw, R. G. and Mitchell-Olds, T. (1993). ANOVA for unbalanced data: an overview. *Ecology* **74**, 1638-1645.
Sokal, R. R. and Rohlf, F. J. (1995). *Biometry: The Principles and Practice of Statistics in Biological Research,* 3rd edn. New York: Freeman and Co.
Surlykke, A., Ghose, K. and Moss, C. F. (2009). Acoustic scanning of natural scenes by echolocation in the big brown bat, *Eptesicus fuscus*. *J. Exp. Biol.* **212**, 1011-1020.
Vittinghoff, E. S. C., Shiboski, D. V., Glidden and McCulloch, C. E. (2005). *Regression Methods in Biostatistics: Linear, Logistic, Survival, and Repeated Measures Models.* New York: Springer.
Zimmer, W. M. X., Johnson, M. P., Madsen, P. T. and Tyack, P. L. (2005a). Echolocation clicks of free-ranging Cuvier's beaked whales (*Ziphius cavirostris*). *J. Acoust. Soc. Am.* **117**, 3919-3927.